

Fig. 5 Side-force coefficient vs stagnation pressure for various Mach numbers for the data from Fig. 2. Reference area and pressure are the lateral projected area of the asymmetry and the exit dynamic pressure.

separate and the entire flow degrades, although the Reynolds number dependence of the effect in this configuration remains to be quantified. On the basis of these data, it is concluded that control of the thruster plenum pressure and exit plane obliquity (including the aforementioned axisymmetric case wherein the sideforce vector may be oriented azimuthally) provides the ability to quickly orient the thrust vector of nongimbal jets.

Acknowledgments

The data in Ref. 2 were acquired while the author was on the faculty of the Department of Aeronautics at the U.S. Naval Postgraduate School. Preparation of this paper was supported by the Aerospace Sciences Directorate of AFOSR and the Office of Basic Energy Sciences, Department of Energy.

References

- ¹Ferri, A., *Elements of Aerodynamics of Supersonic Flows*, The Macmillan Company, 1949, pp. 170-172.
- ²Horais, Brian J., "Vectored Thrust Control," MS Thesis, U.S. Naval Postgraduate School, Monterey, CA, Dec. 1972.

$\vec{v} \times \vec{B}$ and Density Gradient Electric Fields Measured from Spacecraft

J.R. Lilley Jr.,* I. Katz,† and D.L. Cooke*
S-Cubed, LaJolla, California

Nomenclature

e	= electron charge
ℓ	= distance
\vec{v}	= velocity of satellite
\vec{B}	= magnetic field
\vec{E}	= electric field
L	= approximate radius of spacecraft
\vec{F}_L	= Lorentz force
n_i, n_e	= ion, electron density
n_1, n_2	= local ion densities in spacecraft wake
n_0	= undisturbed electron density

Received June 24, 1985; revision received Nov. 5, 1985. Copyright © American Institute of Aeronautics and Astronautics, Inc., 1986. All rights reserved.

*Research Scientist.

†Program Manager. Member AIAA.

ϕ = local potential
 θ_e = electron temperature, V

THE electric fields observed on satellites can be due to a number of environmental influences. Density gradients and $\vec{v} \times \vec{B}$ are two causes of electric fields measured in low earth orbit. The electric fields due to density gradients mainly affect the smaller satellites, while voltages generated by moving through magnetic fields are dominant on larger objects. For spacecraft the size of the Space Shuttle Orbiter (10-30 m), the two effects are of the same order of magnitude. Measurements made during flights of the orbiter support this observation.

When a good conductor moves magnetic field lines, it develops a tangential electric field to cancel the Lorentz force on its conduction electrons. The tangential electric field can be found in the plasma's frame of reference by solving

$$\vec{F}_L = e(\vec{E} + \vec{v} \times \vec{B}) = 0$$

to find

$$\vec{E} = -\vec{v} \times \vec{B} \quad (1)$$

An electric field is also generated by the density gradient found in the wake of a fast-moving spacecraft through a dense plasma. By fast, we mean that the spacecraft is supersonic with respect to the dominant ion species, and by dense, we mean that spacecraft dimensions are large compared with the unperturbed ionospheric plasma Debye length. The Shuttle Orbiter satisfies both these conditions. The potential in the wake can be estimated using quasineutrality and the Boltzmann relation for electrons.

$$n_i \approx n_e$$

$$n_e = n_0 e^{(\phi/\theta_e)}$$

Solving for ϕ

$$\phi = \theta_e \ln(n_e/n_0)$$

the electric field resulting from density gradients can be approximated by the change in the local potential over a length roughly the size of the cross-section of spacecraft with respect to the ram direction. Or

$$\vec{E} \approx -(\Delta\phi/L) \approx -(\phi/L)[\ln(n_2/n_0) - \ln(n_1/n_0)] \quad (2)$$

The magnitude of electric fields due to the two effects can be approximated using Eqs. (1) and (2). Assuming a 10^{11} m^{-3} plasma with a magnetic field of 0.4 G and a density gradient of four orders of magnitude in the wake (as observed on the Shuttle Orbiter) at low altitudes and higher latitudes, we can estimate the magnitude of the electric fields caused by both processes. Using an orbital velocity of 7.7 km/s, the $\vec{v} \times \vec{B}$ field would be 0.31 V/m and independent of vehicle dimensions. Table 1 is for density gradient fields and, as can be seen from Eq. (2), depends inversely on the size of the orbiting spacecraft.

The electric field magnitudes lead one to expect small satellites ($\sim 1-2 \text{ m}$ in diam) to have local fields dominated by density gradient fields and large spacecraft ($\sim 50-200 \text{ m}$, i.e.,

Table 1 Electric fields due to density gradients of four orders of magnitude¹

$L, \text{ m}$	$\theta = 0.1 \text{ eV}$	$\theta = 0.2 \text{ eV}$
	$E, \text{ V/m}$	$E, \text{ V/m}$
0.5	1.8	3.7
5.0	0.18	0.37
50.0	0.018	0.037

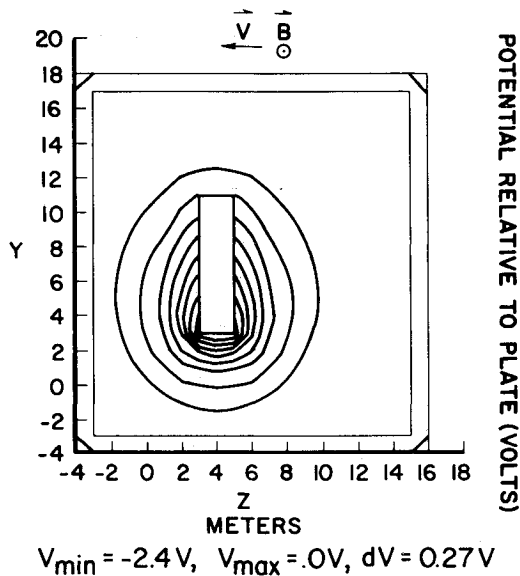


Fig. 1 $8 \times 8 \times 2$ -m plate in low density (1 m^{-3}) plasma. No density gradient electric fields, viewed in the plasma reference frame.

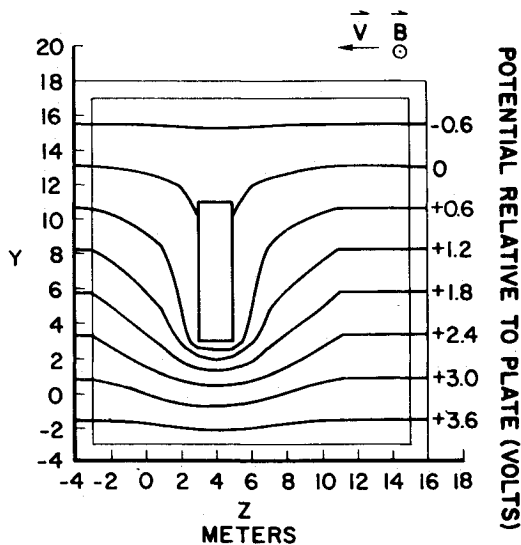


Fig. 2 $8 \times 8 \times 2$ -m plate in same plasma as Fig. 1 viewed in the plate's reference frame.

space stations) to have fields mainly dependent on magnetic field effects. Objects the size of the Space Shuttle (~ 10 - 30 m) will experience electric field contributions of the same order of magnitude from both the Lorentz force and the density gradient fields.

Small satellites have observed electric fields of the order of 1 V/m. Samir et al.² measured these plasma potentials as their probe rotated through the wake of the Atmospheric Explorer-C (AE-C). Measurements made on Orbiter flights have indeed seen electric fields from both influences. Raitt et al.³ recorded $\vec{v} \times \vec{B}$ on the order of the predicted magnitude, where \vec{r} was the distance from the detector to spacecraft ground (the engine nozzle). The potentials they observed correspond to a maximum electric field of roughly 0.4 V/m. Smiddy et al.⁴ measured a density gradient electric field of 0.16 V/m while moving with the detector aligned with the velocity vector.

Computer calculations using the POLAR code⁵ also show the interaction of the two electric fields. POLAR is a three-dimensional spacecraft/environment interaction computer code designed to model the interaction of large objects in the low earth polar orbit. It includes models of spacecraft wakes,

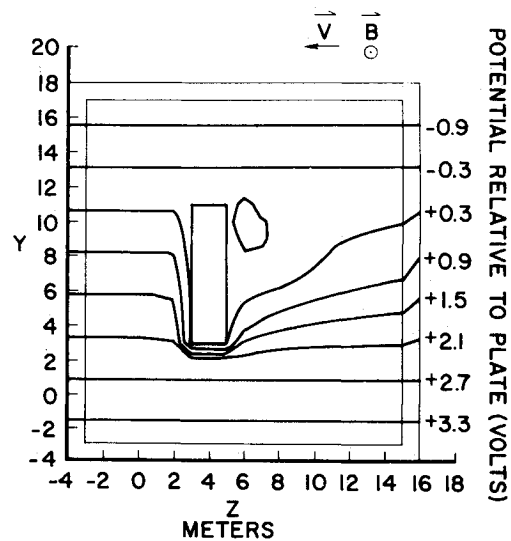


Fig. 3 $8 \times 8 \times 2$ -m plate in high density (10^{12} m^{-3}) plasma as viewed from the plate's reference frame. Both $\vec{v} \times \vec{B}$ and density gradient fields are present in the wake.

magnetic field effects, plasma sheaths, solar auroral particle descriptions and charged particle/surface interactions.⁶

Solutions of the space potentials were calculated self-consistently along with current balance of the ambient plasma to an $8 \times 8 \times 2$ -m metal plate. The plate moved with a Mach vector of $-8\hat{z}$ through a 0.1 eV plasma, typical for non-charging low earth orbit environments. A $-0.4\hat{x}$ G magnetic field was included. To demonstrate the effect of the density gradient electric field, the problem was solved using densities of 1 m^{-3} (vacuum, Figs. 1 and 2) and 10^{12} m^{-3} (low earth orbit environment, Fig. 3).

The magnetic field generated an electric field of -0.25 V/m along the y-axis. The density gradient electric field was found by the code.⁷ Figure 1 shows the potential around the plate due only to $\vec{v} \times \vec{B}$ field in plasma's reference frame. Figure 2 is the same set of potentials as seen in the spacecraft frame. Figure 3 is the same object in the plate's reference frame, with the plasma and density gradient electric fields included. In Fig. 3, the electric fields interact in the wake in an anticipated manner. Note that the $\vec{v} \times \vec{B}$ field is not perturbed by density gradient fields in the ram direction, since the ion density there is almost undisturbed and thus there is no quasineutral electric field, while behind the plate, the electric fields are roughly equivalent.

In conclusion, for Shuttle-sized objects, care must be taken when interpreting measurements of plasma electric fields or space potentials. Plasma parameters, geometrical effects, and velocity effects may obscure the source of observed electric fields.

Acknowledgment

This work supported and performed in cooperation with the Air Force Geophysics Laboratory, Hanscom Air Force Base, Massachusetts, under Contract F19628-82-C-0081.

References

- ¹Murphy, G.B., et al., "Interaction of the Space Shuttle Orbiter with the Ionospheric Plasma," *17th ESLAB Symposium, Spacecraft-Plasma Interactions and Their Influence on Field and Particle Measurements*, Noordwijk, Netherlands, 1983.
- ²Samir, U., Gordon, R., Brace, L., and Theis, R., "The Near-Wake Structure of the Atmosphere Explorer C (AE-C) Satellite: A Parametric Investigation," *Journal of Geophysical Research*, Vol. 84, A2, 1979, pp. 513-525.
- ³Raitt, W.J., Siskind, D.E., Banks, P.M., and Williamson, P.R., "Measurements of the Thermal Plasma Environment of the Space Shuttle," *Planetary and Space Science*, Vol. 32, 1984, pp. 457-467.

⁴Smiddy, M., Sullivan, W.P., Girouard, D., and Anderson, P.J. "Observation of Electric Fields, Electron Densities and Temperature from the Space Shuttle," AIAA Paper 83-2625, Nov. 1983.

⁵Cooke, D.L., Katz, I., Mandell, M.J., Lilley, J.R. Jr., and Rubin, A.J., "A Three-Dimensional Calculation of Shuttle Charging in Polar Orbit," *Spacecraft Environmental Interactions Technology Conference*, Colorado Springs, CO, Oct. 1983.

⁶Cooke, D.L., Lilley, J.R., Jr., and Katz, I., "Preliminary Documentation for the POLAR Code," *Scientific Report No. 1*, SSS-R-83-6027, Oct. 1984.

⁷Katz, I., Cooke, D.L., Parks, D.E., Mandell, M.J., and Rubin, A.G., "Three-Dimensional Wake Model for Low Earth Orbit," *Journal of Spacecraft and Rockets*, Vol. 21, Jan.-Feb. 1984, pp. 125-127.

Comparison of Methane and Propane Rockets

James A. Martin*

NASA Langley Research Center, Hampton, Virginia

Introduction

THE potential benefits of hydrocarbon fuels and dual-fuel propulsion for future Earth-to-orbit vehicles have been shown in a number of studies.¹⁻⁶ Of the several hydrocarbon fuels considered, methane and propane are the favored candidates. In a previous study,⁵ methane and propane were compared for use in a single-stage, Earth-to-orbit vehicle with dual-fuel rocket propulsion. The results indicated a significant advantage for propane, and further optimizations were conducted using this fuel. The purpose of this Note is to show how the comparison changes when both methane and propane vehicles are optimized. The analysis is the same as that described in Ref. 5.

Results

The results are shown in Figs. 1 and 2. In Fig. 1, the dry mass characteristics of vehicles with both fuels are shown. The flagged symbols at a hydrocarbon thrust fraction of 0.8 and a hydrocarbon propellant fraction of 0.79 are the same results shown in preliminary screening.⁵ As the vehicles are optimized, the difference is reduced slightly, but the conclusions do not change. Propane is still the preferred hydrocarbon fuel to

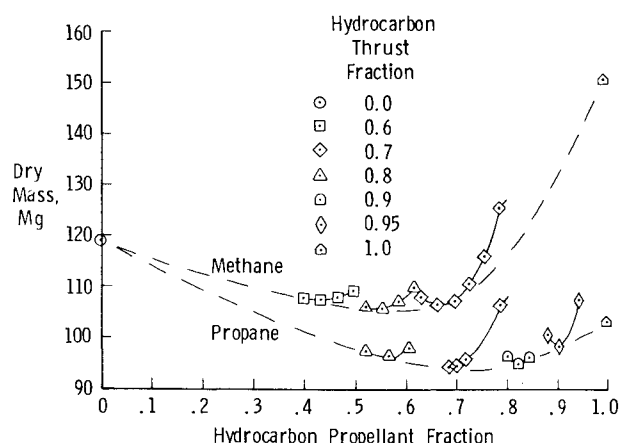


Fig. 1 Effect of fuel on vehicle dry-mass optimization.

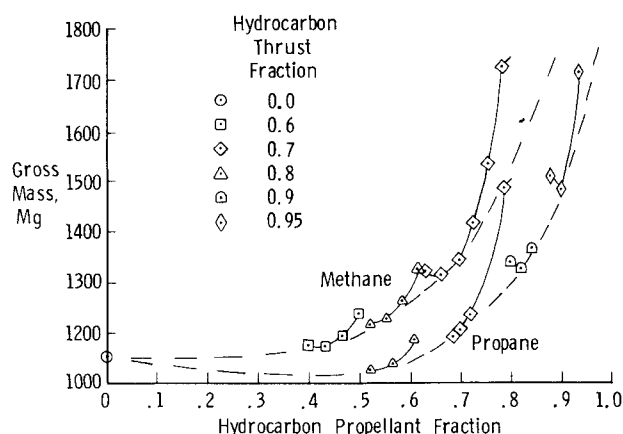


Fig. 2 Effect of fuel on vehicle gross-mass optimization.

minimize dry mass. Figure 2 shows the corresponding results for vehicle gross mass. In this figure, the difference between propane and methane decreases noticeably when moving from the flagged symbols to the points with minimum gross mass. Propane is the fuel which minimizes gross mass. The results with methane indicate that a vehicle with only hydrogen fuel (a hydrocarbon fuel fraction of 0.0) has a gross mass as low as any dual-fuel vehicle.

Conclusion

When single-stage-to-orbit vehicles with methane and propane fueled rockets are optimized, the preferred fuel for minimum dry or gross mass is propane.

References

- ¹Salkeld, R., "Single-Stage Shuttles for Ground Launch and Air Launch," *Aeronautics and Astronautics*, Vol. 12, March 1974, pp. 52-64.
- ²Haefeli, R.C., Littler, E.G., Hurley, J.R., and Winter, M.G., "Technology Requirements for Advanced Earth-Orbital Transportation Systems, Dual-Mode Propulsion," NASA CR-2868, June 1977.
- ³Wilhite, A.W., "Optimization of Rocket Propulsion Systems for Advanced Earth-to-Orbit Shuttles," *Journal of Spacecraft and Rockets*, Vol. 17, March-April 1980, pp. 99-104.
- ⁴Caluori, V.A., Conrad, R.J., and Jenkins, J.C., "Technology Requirements for Future Earth-to-Geosynchronous Orbit Transportation Systems," NASA CR 3265, April 1980.
- ⁵Martin, J.A., "Hydrocarbon Rocket Engines for Earth-to-Orbit Vehicles," *Journal of Spacecraft and Rocket*, Vol. 20, May-June 1983, pp. 249-256.
- ⁶Martin, J.A., Naftel, J.C., and Turriziani, R.V., "Propulsion Evaluation for Orbit-on-Demand Vehicles," AIAA Paper 85-1161, July 1985.

Second-Order Roll Damping of Rolling Wings at Supersonic Speeds

Weikai Gu*

Academia Sinica, Beijing, China

Nomenclature

- b = wing span
 $B = (M^2 - 1)^{1/2}$

Received Aug. 10, 1985; revision submitted Nov. 15, 1985. Copyright © American Institute of Aeronautics and Astronautics, Inc., 1986. All rights reserved.

*Research Associate, Aerodynamics Division, Institute of Mechanics.

Received Oct. 28, 1985; revision received Jan. 10, 1986. This paper is declared a work of the U.S. Government and is not subject to copyright protection in the United States.

*Aerospace Engineer, Space Systems Division. Associate Member AIAA.